


RESEARCH ARTICLE | OCTOBER 06 2023

## NMC cathode precursor synthesis by hydroxide co-precipitation method: A mini review

Muhammad Fakhrudin ; Evvy Kartini



AIP Conf. Proc. 2932, 020007 (2023)

<https://doi.org/10.1063/5.0174823>



CrossMark

### Articles You May Be Interested In

Completing the dark matter solutions in degenerate Kaluza-Klein theory

*J. Math. Phys.* (April 2019)

Gibbs measures based on 1d (an)harmonic oscillators as mean-field limits

*J. Math. Phys.* (April 2018)

An upper diameter bound for compact Ricci solitons with application to the Hitchin–Thorpe inequality. II

*J. Math. Phys.* (April 2018)

500 kHz or 8.5 GHz?  
And all the ranges in between.

Lock-in Amplifiers for your periodic signal measurements



Find out more



# NMC Cathode Precursor Synthesis by Hydroxide Coprecipitation Method: A Mini Review

Muhammad Fakhrudin<sup>1, 2, a)</sup> and Evvy Kartini<sup>1, 2, b)</sup>

<sup>1</sup> *Research Center for Advanced Material, Research Organization for Nanotechnology and Materials, National Research, and Innovation Agency (BRIN), Kawasan PUSPIPTEK, Serpong, Tangerang Selatan, Banten 15314, Indonesia.*

<sup>2</sup> *National Battery Research Institute, Indonesian Life Science Center, Technology Business Zone BRIN Puspiptek Area, Bogor, 16340, West Java, Indonesia.*

<sup>a)</sup> *Corresponding author: muha202@brin.go.id*

<sup>b)</sup> *evvy001@brin.go.id*

**Abstract.** Morphological properties of cathode precursors greatly affect the performance of the final product of the active cathode material. The precursor acts as a template of the cathode because of the ability to maintain its morphology during calcination with lithium. To produce precursors with appropriate specifications, several key parameters of the coprecipitation reaction must be carefully regulated, such as pH, ammonia concentration, stirring rate, temperature, and reaction time. In this review, the crucial parameters of widely applied hydroxide coprecipitation will be discussed regarding their impact on the development of mixed hydroxide precursor.

## INTRODUCTION

The need for batteries as energy storage for electric vehicles is increasing along with the increasing market demand. Batteries with high energy density, high cycle life, and high safety are still being demanded to improve so that electric vehicles can completely replace Internal Combustion Engine (ICE) vehicles. One of the battery components that determine the performance as well as the cost is the cathode material [1]–[7]. In terms of capacity, the current cathode has not been able to compete with the energy density of the conventional graphite anode [8]. While the cost itself contributes 30–45% of the battery cells' price [9]–[11].

One of the most popular cathode materials nowadays, layered oxide NMC ( $\text{LiNi}_x\text{Mn}_y\text{Co}_z\text{O}_2$ ,  $x+y+z=1$ ), has practical energy densities of 200–230 mAh  $\text{g}^{-1}$  [11]. NMC cathode is composed of a mixture of transition metals (TM): Nickel, Manganese, and Cobalt. The composition of Ni determines the capacity, Mn stabilizes the structure, and Co increases the electronic conductivity thereby increasing the rate performance [13–14]. Optimization of cathode synthesis with these three transition metal compositions is very challenging because the way we mix and form the crystal structure will greatly affect its performance [14]–[19].

Some of the known transition metal oxide cathode synthesis methods are sol-gel, solid-state, spray pyrolysis, and coprecipitation [19]–[21]. The most widely applied in industry is coprecipitation because it offers easy scaling-up, high transition metal mixing, and moderate cost [22]. The coprecipitation method is carried out by simultaneously precipitating transition metal ions in the solution with the help of precipitating and chelating agents [19], [23], [24]. Hydroxide precipitating agents are widely used because they produce hydroxide precipitate products, called precursors, which have high tap density, narrow particle size distribution, and ease of particle morphology control [25]. In this paper, the hydroxide coprecipitation process to synthesize precursors based on previous findings will be presented completely and concisely. Parameters such as pH, ammonia concentration, temperature, reaction time, and others will be discussed regarding their effect on the formation of mixed hydroxide precursor precipitate. This review is expected to be a brief reference before selecting the parameters of the coprecipitation process.

## METHODOLOGY

This review was carried out by collecting all the information related to the hydroxide coprecipitation reaction. The scope of the literature is limited to cathode types of NMC but does not limit the discussion of co-precipitation of other cathode types for comparison, such as NCA, NMCA and others.

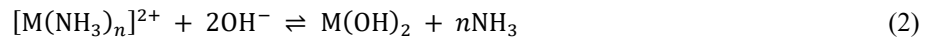
## RESULTS AND DISCUSSION

### Reactant preparation and reaction setup

Conventional co-precipitation reaction of mixed metal hydroxide is commonly conducted in a continuous stirred tank reactor (CSTR) as shown in Fig. 1(a). Solution of TM, commonly sulfate salt, and NaOH as the precipitating agent was dissolved in deionized water. A 2 and 4 mol/l concentration of TM and NaOH, respectively, is generally used. Higher concentration is avoided because of the possibility of causing local supersaturation.  $\text{NH}_3$  chelating agent was available on the market in concentrated aqueous solution and need to be diluted into lower concentration. To ensure that there is no dissolved oxygen, the solutions should be boiled for several minutes [26]–[28]. Each solution is pumped separately into the reactor. As TM and  $\text{NH}_3$  solution is pumped steadily at a certain ratio, the flowing of NaOH solution was regulated by a pH controller to maintain a certain pH value in the reactor. The solution mixture in the reactor was stirred vigorously by an impeller controlled by a motor speed controller. The inert gas,  $\text{N}_2$  or Ar, was bubbled through the reactor to expel and ensure there is no  $\text{O}_2$  in the CSTR along the reaction. Slurry product was collected through an overflowing pipe in the continuous co-precipitation mode.

### Reaction mechanism

The reaction mechanism is shown in Equation 1-3 where  $\text{M}^{2+}$  indicates Ni, Mn, and Co ions in solution. In hydroxide co-precipitation,  $\text{NH}_3$  as a chelating agent is needed to slow down the precipitation reaction through ammonia complexation reaction as shown in Eq. (1). With this complexation, the particle size of the hydroxide precipitate according to Eq. (2) can be controlled so that the size distribution becomes narrower. It is an equilibrium equation where the dissolution-recrystallization process occurs so that a spherical morphology is produced [26]. Due to the presence of hydroxide ions at high pH, the surface of the precursor particles will be negatively charged through the proton abstraction reaction in Eq. (3). This negatively charged particle surface prevents agglomeration through repulsion between particles [29].



### Particle growth mechanism

In the early stage of co-precipitation, nucleation occurs due to supersaturation where the saturated solution will start to form nuclei, or what we call primary particles on the nanometer scale [26], [28], [30]. Each of the primary particles will grow to a larger size, generally in the submicron range [29]. Nucleus crystal growth will follow the orientation of the initial crystal nucleus so that the primary particles are still in the form of a single crystal. Then the primary particles collide with each other, stick to each other with random orientations, and agglomeration occurs so that the so-called secondary particles are polycrystalline [25], [30].

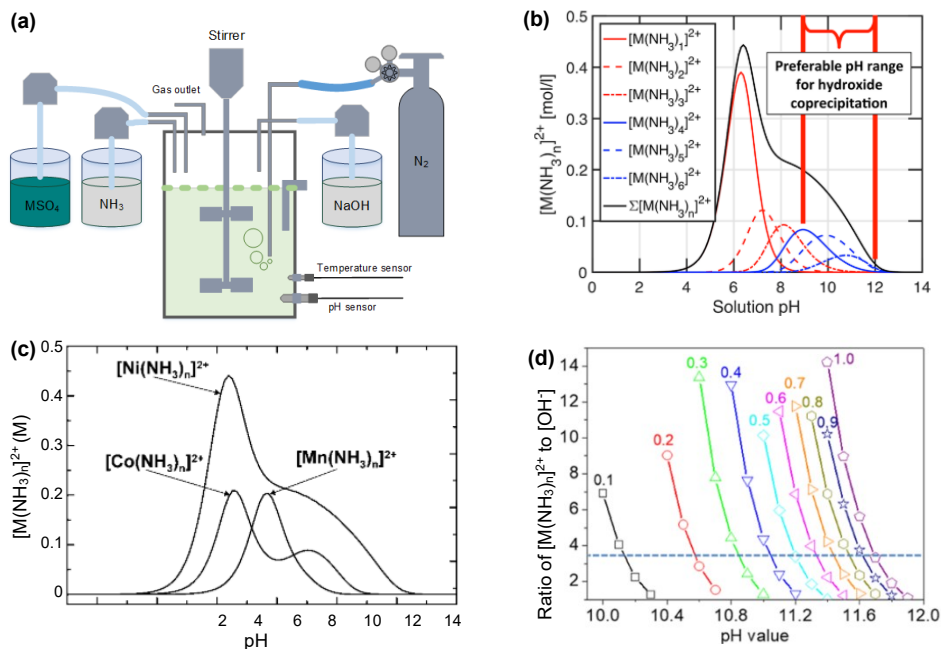


**FIGURE 1.** (a) CSTR equipment setup; (b) Concentration of ammonia complex in different pH values. Reprinted (adapted) with permission from [29] © 2019 American Chemical Society; (c) Concentration of specific metal-ammonia complex in different pH values. Reprinted (adapted) with permission from [26] © 2009 American Chemical Society; (d) Map of pH and  $\text{NH}_3$  concentration that gives the ratio of metal ammonia complex to  $[\text{OH}^-]$  3.4. Reprinted (adapted) with permission from [25] © 2021 American Chemical Society.

### Effect of pH and Ammonia amount

The involvement of metal ammonia complex compounds in Eq. (1) and (2) can be influenced by the pH value so pH regulation is very necessary. The appropriate pH value will control the amount of complex compound required. By solving the equilibrium and mass balance equations for the metal-ammonia complexation reaction, Barai et al provided profiles of metal-ammonia complexes concentration in different pH values as shown in Fig. 1(b)[29]. To ensure the number of hydroxide ions during the reaction, the pH of the general coprecipitation is set to more than 9. From Fig. 1 (b) we can see that at a pH of more than 12, the number of complex compounds is very small so the coprecipitation reaction should be carried out in the pH range of 9-12. However, Figure 1(b) was based on the assumption that the transition metals Ni, Mn, and Co, have the same equilibrium values for the complexation reactions. Van Bommel et al calculated the metal-ammonia complex concentration for each metal in Figure 1(c) [26]. Ni can coordinate with ammonia up to pH 12, while Mn and Co are only up to pH 10. This is in accordance with experimental results where the optimal pH for coprecipitation of lower Ni-containing hydroxide which produces high tap density is lower [25], [26]

The effect of pH on particle morphology has been widely reported. Increasing the pH will increase the amount of  $\text{OH}^-$  so that the supersaturation increases. This causes the rate of nucleation and crystal growth to increase. However, at a certain pH value, the nucleation rate will increase rapidly beyond the crystal growth rate so that many small nuclei are formed. Ding et al demonstrated that co-precipitation of  $\text{Ni}_{0.8}\text{Mn}_{0.1}\text{Co}_{0.1}(\text{OH})_2$  at higher pH of 12 produced colloidal particles because the particle size was too small. These small particles will easily agglomerate when drying and have a low tap density [15]. While at lower pH, 10.5, the secondary particles agglomerated which caused a wide distribution and large particle size. Optimal results were achieved when the pH was set to a value of 11.2 which resulted in high sphericity and uniformity particles. Vu et al also optimized the pH value for precursor synthesis of NMC811 and found that the optimum pH was 11.5 [31].

The difference in the optimum pH value, apart from being influenced by the composition of the transition metal, is also influenced by the amount of ammonia. The higher the concentration of ammonia, the more metal complexes formed so that supersaturation decreases and limits the rate of nucleation. Restricted nucleation will encourage nucleus

crystals to grow and agglomeration to form secondary particles will be facilitated. Too low  $\text{NH}_3$  will cause the nucleation rate to increase and irregular small particles will be formed instead of the uniform spherical particle [31]–[34]. Meanwhile, too high  $\text{NH}_3$  will result in too many complex ions being formed so that not all  $\text{M}^{2+}$  ions are precipitated thus TM composition deviations occur in the precursor [15], [16], [32], [34].

Since both pH and  $\text{NH}_3$  affect Eq. (1) and (2), general rules for obtaining optimal morphology have been proposed by Shen et al [32]. They proposed that to get a good particle morphology, the ratio of the concentration of metal complexes to the concentration of  $\text{OH}^-$  should be 3.4. A mapping of pH and  $\text{NH}_3$  concentration with the proposed ratio was given in Fig. 1 (d). For example, co-precipitation at 1 mol/l  $\text{NH}_3$  should be conducted at pH 11.7, as for low  $\text{NH}_3$  of 0.1 mol/l the pH should be 10.1. It should be noted here that this general rule gives a slightly larger particle size at a smaller selected pH value, while the tap density will increase significantly at high pH concentrations.

### **Effect of Temperature**

In general, an increase in temperature will increase the reaction rate. However, the presence of manganese limits the application of temperatures higher than 60 °C because of its high potential to easily oxidize manganese to  $\text{MnOOH}$  [31], [35],  $\text{MnO}(\text{OH})_2$  [33],  $\text{MnO}_2$  [36], or  $\text{Mn}_3\text{O}_4$  [31]. Hydroxide coprecipitation is generally carried out at 50–60 °C [33], [34]. Liang et al synthesized NMC811 by varying the temperature and found that in the 50–60°C temperature range had no significant morphological difference, with the highest tap density obtained at 55 °C. Vu et al also reported that increasing the temperature from 45 to 50°C can change the shape of the primary particles from needle-like to plate-like, thus increasing the tap density [31]. Coprecipitation at room temperature has also been investigated by Cheng et al under pH 9 for 1 hour [14]. Regardless of the short reaction time used, the reaction at room temperature is likely to slow down the formation of secondary spherical particles as the SEM results show that the particles are irregular and agglomerated.

### **Effect of reaction time**

As indicated in various literature, the optimal reaction time may vary according to the material composition and operating conditions. The reported reaction times for  $\text{Ni}_{1/3}\text{Mn}_{1/3}\text{Co}_{1/3}(\text{OH})_2$  were 12 [37], 20 [38], and 24 hours [39], [40]. As for the Ni-rich  $\text{Ni}_{0.8}\text{Mn}_{0.1}\text{Co}_{0.1}(\text{OH})_2$  was 10 [31], 12 [15], and 20 hours [41].  $\text{Ni}_{0.9}\text{Co}_{0.1}(\text{OH})_2$  with higher Ni content was reported to need 30 hours of reaction times [42], [43]. Generally, the higher the nickel content, the longer it takes to produce precursor particles with a high tap density and narrow size distribution.

### **Effect of stirring speed**

In general, a higher stirring speed will promote the dispersion of reactants thereby avoiding local supersaturation concentrations. Friction between particles and particles with reactor walls will polish the particles to produce smooth surfaces and high sphericity particles [15]. Optimum stirring speed has been reported in the range of 800–1000 rpm [15], [17], [33], [35], [37], [44].

## **CONCLUSION**

Producing high-quality cathode precursors requires careful adjustment of the core parameters of the reaction such as pH,  $\text{NH}_3$  concentration, temperature, stirring speed, etc. The optimal value of each parameter has been discussed and can be used as a guide. However, the slightest difference in equipment setup will greatly affect the formation of precursor morphology. So that whatever has been described previously is only used as an initial reference in carrying out the synthesis. Parameter optimization still must be done to ensure the precursor product is in accordance with the specifications required.

## **ACKNOWLEDGMENTS**

This work was supported by National Battery Research Institute and Research and Innovation Agency (BRIN) of Indonesia.

## REFERENCES

1. A. Chakraborty *et al.*, “Layered Cathode Materials for Lithium-Ion Batteries: Review of Computational Studies on  $\text{LiNi}_{1-x}\text{Co}_x\text{Mn}_y\text{O}_2$  and  $\text{LiNi}_{1-x}\text{Co}_x\text{Al}_y\text{O}_2$ ,” *Chem. Mater.*, vol. 32, no. 3, pp. 915–952, 2020, doi: 10.1021/acs.chemmater.9b04066.
2. Y. Lu, Y. Zhang, Q. Zhang, F. Cheng, and J. Chen, “Recent advances in Ni-rich layered oxide particle materials for lithium-ion batteries,” *Particuology*, vol. 53, pp. 1–11, 2020, doi: 10.1016/j.partic.2020.09.004.
3. X. Xu, S. Lee, S. Jeong, Y. Kim, and J. Cho, “Recent progress on nanostructured 4 v cathode materials for Li-ion batteries for mobile electronics,” *Mater. Today*, vol. 16, no. 12, pp. 487–495, 2013, doi: 10.1016/j.mattod.2013.11.021.
4. N. Voronina, Y. K. Sun, and S. T. Myung, “Co-Free Layered Cathode Materials for High Energy Density Lithium-Ion Batteries,” *ACS Energy Lett.*, vol. 5, no. 6, pp. 1814–1824, 2020, doi: 10.1021/acseenergylett.0c00742.
5. J. U. Choi, N. Voronina, Y. K. Sun, and S. T. Myung, “Recent Progress and Perspective of Advanced High-Energy Co-Less Ni-Rich Cathodes for Li-Ion Batteries: Yesterday, Today, and Tomorrow,” *Adv. Energy Mater.*, vol. 10, no. 42, pp. 1–31, 2020, doi: 10.1002/aenm.202002027.
6. N. Mohamed and N. K. Allam, “Recent advances in the design of cathode materials for Li-ion batteries,” *RSC Adv.*, vol. 10, no. 37, pp. 21662–21685, 2020, doi: 10.1039/d0ra03314f.
7. F. Schipper, E. M. Erickson, C. Erk, J.-Y. Shin, F. F. Chesneau, and D. Aurbach, “Review—Recent Advances and Remaining Challenges for Lithium Ion Battery Cathodes,” *J. Electrochem. Soc.*, vol. 164, no. 1, pp. A6220–A6228, 2017, doi: 10.1149/2.0351701jes.
8. B. Zhu, X. Wang, P. Yao, J. Li, and J. Zhu, “Towards high energy density lithium battery anodes: Silicon and lithium,” *Chem. Sci.*, vol. 10, no. 30, pp. 7132–7148, 2019, doi: 10.1039/c9sc01201j.
9. R. V. Salvatierra, W. Chen, and J. M. Tour, “What Can be Expected from ‘Anode-Free’ Lithium Metal Batteries?,” *Adv. Energy Sustain. Res.*, vol. 2, no. 5, p. 2000110, 2021, doi: 10.1002/aesr.202000110.
10. K. Lu, C. Zhao, and Y. Jiang, “Research progress of cathode materials for lithium-ion batteries,” *E3S Web Conf.*, vol. 233, 2021, doi: 10.1051/e3sconf/202123301020.
11. M. Greenwood, M. Wentker, and J. Leker, “A bottom-up performance and cost assessment of lithium-ion battery pouch cells utilizing nickel-rich cathode active materials and silicon-graphite composite anodes,” *J. Power Sources Adv.*, vol. 9, no. December 2020, p. 100055, 2021, doi: 10.1016/j.powera.2021.100055.
12. R. Ma *et al.*, “Tuning Cobalt-Free Nickel-Rich Layered  $\text{LiNi}_0.9\text{Mn}_0.1\text{O}_2$  Cathode Material for Lithium-Ion Batteries,” *ChemElectroChem*, vol. 7, no. 12, pp. 2637–2642, 2020, doi: 10.1002/celec.202000443.
13. L. Xu *et al.*, “Progress in Preparation and Modification of  $\text{LiNi}_0.6\text{Mn}_0.2\text{Co}_0.2\text{O}_2$  Cathode Material for High Energy Density Li-Ion Batteries,” *Int. J. Electrochem.*, vol. 2018, pp. 1–12, 2018, doi: 10.1155/2018/6930386.
14. C. Cheng, L. Tan, H. Liu, and X. Huang, “High rate performances of the cathode material  $\text{LiNi}_{1/3}\text{Co}_{1/3}\text{Mn}_{1/3}\text{O}_2$  synthesized using low temperature hydroxide precipitation,” *Mater. Res. Bull.*, vol. 46, no. 11, pp. 2032–2035, 2011, doi: 10.1016/j.materresbull.2011.07.004.
15. Y. Ding, D. Mu, B. Wu, Z. Zhao, and R. Wang, “Controllable synthesis of spherical precursor  $\text{Ni}_0.8\text{Co}_0.1\text{Mn}_0.1(\text{OH})_2$  for nickel-rich cathode material in Li-ion batteries,” *Ceram. Int.*, vol. 46, no. 7, pp. 9436–9445, 2020, doi: 10.1016/j.ceramint.2019.12.204.
16. Y. Shen *et al.*, “A highly promising high-nickel low-cobalt lithium layered oxide cathode material for high-performance lithium-ion batteries,” *J. Colloid Interface Sci.*, vol. 597, pp. 334–344, 2021, doi: 10.1016/j.jcis.2021.04.008.
17. M. Noh and J. Cho, “Optimized Synthetic Conditions of  $\text{LiNi}_{0.5}\text{Co}_{0.2}\text{Mn}_{0.3}\text{O}_2$  Cathode Materials for High Rate Lithium Batteries via Co-Precipitation Method,” *J. Electrochem. Soc.*, vol. 160, no. 1, pp. A105–A111, 2013, doi: 10.1149/2.004302jes.
18. S. H. Lee, K. Y. Kwon, B. K. Choi, and H. D. Yoo, “A kinetic descriptor to optimize Co-precipitation of Nickel-rich cathode precursors for Lithium-ion batteries,” *J. Electroanal. Chem.*, vol. 924, no. September, p. 116828, 2022, doi: 10.1016/j.jelechem.2022.116828.
19. M. Fakhrudin and E. Kartini, “La-incorporated NMC811 as a new Li-ion battery cathode material,” *Int. Conf. Adv. Mater. Technol. 2021*, vol. 2708, no. November, p. 070003, 2022, doi: 10.1063/5.0123495.
20. M. Malik, K. H. Chan, and G. Azimi, “Review on the synthesis of  $\text{LiNi}_x\text{Mn}_y\text{Co}_{1-x-y}\text{O}_2$  (NMC) cathodes for lithium-ion batteries,” *Mater. Today Energy*, vol. 28, p. 101066, 2022, doi: 10.1016/j.mtener.2022.101066.
21. E. Kartini, M. Fakhrudin, W. Astuti, S. Sumardi, and M. Z. Mubarak, “The study of  $(\text{Ni},\text{Mn},\text{Co})\text{SO}_4$  as raw

- material for NMC precursor in lithium ion battery,” *Int. Conf. Adv. Mater. Technol. 2021*, vol. 2708, no. November, p. 070001, 2022, doi: 10.1063/5.0122596.
22. S. Ahmed, P. A. Nelson, K. G. Gallagher, N. Susarla, and D. W. Dees, “Cost and energy demand of producing nickel manganese cobalt cathode material for lithium ion batteries,” *J. Power Sources*, vol. 342, pp. 733–740, 2017, doi: 10.1016/j.jpowsour.2016.12.069.
  23. D. F. Fadrian and M. Wahyu, “material prepared via carbonate co- precipitation method Via Carbonate Co-Precipitation Method,” vol. 070004, no. November, pp. 4–9, 2022.
  24. M. W. S. Mubarak, M. Fakhruddin, and E. Kartini, “Ce-doped NMC 811 synthesis as cathode material,” *Int. Conf. Adv. Mater. Technol. 2021*, vol. 2708, no. November, p. 070006, 2022, doi: 10.1063/5.0122599.
  25. Y. Yang, S. Xu, M. Xie, Y. He, G. Huang, and Y. Yang, “Growth mechanisms for spherical mixed hydroxide agglomerates prepared by co-precipitation method: A case of Ni<sub>1/3</sub>Co<sub>1/3</sub>Mn<sub>1/3</sub>(OH)<sub>2</sub>,” *J. Alloys Compd.*, vol. 619, pp. 846–853, 2015, doi: 10.1016/j.jallcom.2014.08.152.
  26. A. Van Bommel and J. R. Dahn, “Analysis of the growth mechanism of coprecipitated spherical and dense nickel, manganese, and cobalt-containing hydroxides in the presence of aqueous ammonia,” *Chem. Mater.*, vol. 21, no. 8, pp. 1500–1503, 2009, doi: 10.1021/cm803144d.
  27. J. Li, H. Li, W. Stone, R. Weber, S. Hy, and J. R. Dahn, “Synthesis of Single Crystal LiNi<sub>0.5</sub> Mn<sub>0.3</sub> Co<sub>0.2</sub> O<sub>2</sub> for Lithium Ion Batteries,” *J. Electrochem. Soc.*, vol. 164, no. 14, pp. A3529–A3537, 2017, doi: 10.1149/2.0401714jes.
  28. M. L. Para *et al.*, “A modelling and experimental study on the co-precipitation of Ni<sub>0.8</sub>Mn<sub>0.1</sub>Co<sub>0.1</sub>(OH)<sub>2</sub> as precursor for battery cathodes,” *Chem. Eng. Sci.*, vol. 254, p. 117634, 2022, doi: 10.1016/j.ces.2022.117634.
  29. P. Barai, Z. Feng, H. Kondo, and V. Srinivasan, “Multiscale Computational Model for Particle Size Evolution during Coprecipitation of Li-Ion Battery Cathode Precursors,” *J. Phys. Chem. B*, vol. 123, no. 15, pp. 3291–3303, 2019, doi: 10.1021/acs.jpcc.8b12004.
  30. X. Yang *et al.*, “Growth mechanisms for spherical Ni<sub>0.815</sub>Co<sub>0.15</sub>Al<sub>0.035</sub>(OH)<sub>2</sub> precursors prepared via the ammonia complexation precipitation method,” *J. Energy Chem.*, vol. 53, pp. 379–386, 2020, doi: 10.1016/j.jechem.2020.05.049.
  31. D. L. Vu and J. won Lee, “Properties of LiNi<sub>0.8</sub>Co<sub>0.1</sub>Mn<sub>0.1</sub>O<sub>2</sub> as a high energy cathode material for lithium-ion batteries,” *Korean J. Chem. Eng.*, vol. 33, no. 2, pp. 514–526, 2016, doi: 10.1007/s11814-015-0154-3.
  32. Y. Shen *et al.*, “Insight into the Coprecipitation-Controlled Crystallization Reaction for Preparing Lithium-Layered Oxide Cathodes,” *ACS Appl. Mater. Interfaces*, vol. 13, no. 1, pp. 717–726, 2021, doi: 10.1021/acsmi.0c19493.
  33. L. Liang *et al.*, “Co-precipitation synthesis of Ni<sub>0.6</sub>Co<sub>0.2</sub>Mn<sub>0.2</sub>(OH)<sub>2</sub> precursor and characterization of LiNi<sub>0.6</sub>Co<sub>0.2</sub>Mn<sub>0.2</sub>O<sub>2</sub> cathode material for secondary lithium batteries,” *Electrochim. Acta*, vol. 130, pp. 82–89, 2014, doi: 10.1016/j.electacta.2014.02.100.
  34. K. H. Hu *et al.*, “Insight into the evolution of precursor and electrochemical performance of Ni-rich cathode modulated by ammonia during hydroxide precipitation,” *J. Alloys Compd.*, vol. 803, pp. 538–545, 2019, doi: 10.1016/j.jallcom.2019.06.309.
  35. H. J. Jeon, S. A. Monim, C. S. Kang, and J. T. Son, “Synthesis of Li<sub>x</sub>[Ni<sub>0.225</sub>Co<sub>0.125</sub>Mn<sub>0.65</sub>O<sub>2</sub>] as a positive electrode for lithium-ion batteries by optimizing its synthesis conditions via a hydroxide co-precipitation method,” *J. Phys. Chem. Solids*, vol. 74, no. 9, pp. 1185–1195, 2013, doi: 10.1016/j.jpcs.2013.02.006.
  36. H. Qiu, Y. Wang, and S. Ye, “Rationally-Directed Synthesis and Characterization of Nickel-Rich Cathode Material for Lithium Ion Battery,” *Energy Technol.*, vol. 6, no. 12, pp. 2419–2428, 2018, doi: 10.1002/ente.201800415.
  37. M. H. Lee, Y. J. Kang, S. T. Myung, and Y. K. Sun, “Synthetic optimization of Li[Ni<sub>1/3</sub>Co<sub>1/3</sub>Mn<sub>1/3</sub>]O<sub>2</sub> via co-precipitation,” *Electrochim. Acta*, vol. 50, no. 4, pp. 939–948, 2004, doi: 10.1016/j.electacta.2004.07.038.
  38. A. van Bommel and J. R. Dahn, “Synthesis of Spherical and Dense Particles of the Pure Hydroxide Phase Ni<sub>1/3</sub>Mn<sub>1/3</sub>Co<sub>1/3</sub>(OH)<sub>2</sub>,” *J. Electrochem. Soc.*, vol. 156, no. 5, p. A362, 2009, doi: 10.1149/1.3079366.
  39. X. Luo, X. Wang, L. Liao, X. Wang, S. Gamboa, and P. J. Sebastian, “Effects of synthesis conditions on the structural and electrochemical properties of layered Li[Ni<sub>1/3</sub>Co<sub>1/3</sub>Mn<sub>1/3</sub>]O<sub>2</sub> cathode material via the hydroxide co-precipitation method LIB SCITECH,” *J. Power Sources*, vol. 161, no. 1, pp. 601–605, 2006, doi: 10.1016/j.jpowsour.2006.03.090.
  40. S. Zhang, “Characterization of high tap density Li[Ni<sub>1/3</sub>Co<sub>1/3</sub>Mn<sub>1/3</sub>]O<sub>2</sub> cathode material synthesized via hydroxide co-precipitation,” *Electrochim. Acta*, vol. 52, no. 25, pp. 7337–7342, 2007, doi:

- 10.1016/j.electacta.2007.06.015.
41. J. Zeng *et al.*, “F-Doped Ni-Rich Layered Cathode Material with Improved Rate Performance for Lithium-Ion Batteries,” *Processes*, vol. 10, no. 8, 2022, doi: 10.3390/pr10081573.
  42. H. Zhu, H. Yu, H. Jiang, Y. Hu, H. Jiang, and C. Li, “High-efficiency Mo doping stabilized LiNi<sub>0.9</sub>Co<sub>0.1</sub>O<sub>2</sub> cathode materials for rapid charging and long-life Li-ion batteries,” *Chem. Eng. Sci.*, vol. 217, p. 115518, 2020, doi: 10.1016/j.ces.2020.115518.
  43. H. Zhu, H. Yu, Z. Yang, H. Jiang, and C. Li, “Tungsten and phosphate polyanion co-doping of Ni-ultrahigh cathodes greatly enhancing crystal structure and interface stability,” *Chinese J. Chem. Eng.*, vol. 37, pp. 144–151, 2021, doi: 10.1016/j.cjche.2021.04.001.
  44. L. Xu, F. Zhou, J. Kong, Z. Chen, and K. Chen, “Synthesis of Li(Ni<sub>0.6</sub>Co<sub>0.2</sub>Mn<sub>0.2</sub>)O<sub>2</sub> with sodium DL-lactate as an eco-friendly chelating agent and its electrochemical performances for lithium-ion batteries,” *Ionics (Kiel)*, vol. 24, no. 8, pp. 2261–2273, 2018, doi: 10.1007/s11581-017-2363-8.